The Journal of Immunology

TLR4 Signaling Shapes B Cell Dynamics via MyD88-Dependent Pathways and Rac GTPases

Laura Barrio, Julia Saez de Guinoa and Yolanda R. Carrasco

J Immunol 2013; 191:3867-3875; Prepublished online 30 August 2013;
doi: 10.4049/jimmunol.1301623
http://www.jimmunol.org/content/191/7/3867

The Journal of Immunology is published twice each month by
The American Association of Immunologists, Inc.,
1451 Rockville Pike, Suite 650, Rockville, MD 20852

Print ISSN: 0022-1767 Online ISSN: 1550-6606.

TLR4 Signaling Shapes B Cell Dynamics via MyD88-Dependent Pathways and Rac GTPases

Laura Barrio, Julia Saez de Guinoa, and Yolanda R. Carrasco

B cells use a plethora of TLR to recognize pathogen-derived ligands. These innate signals have an important function in the B cell adaptive immune response and modify their trafficking and tissue location. The direct role of TLR signaling on B cell dynamics nonetheless remains almost entirely unknown. In this study, we used a state-of-the-art two-dimensional model combined with real-time microscopy to study the effect of TLR4 stimulation on mouse B cell motility in response to chemokines. We show that a minimum stimulation period is necessary for TLR4 modification of B cell behavior. TLR4 stimulation increased B cell polarization, migration, and directionality; these increases were dependent on the MyD88 signaling pathway and did not require ERK or p38 MAPK activity downstream of TLR4. In addition, TLR4 stimulation enhanced Rac GTPase activity and promoted sustained Rac activation in response to chemokines. These results increase our understanding of the regulation of B cell dynamics by innate signals and the underlying molecular mechanisms. ***The Journal of Immunology*****, 2013, 191: 3867–3875.**

B cells are central elements in the adaptive immune response to pathogens. Ag recognition through the BCR drives B cell activation and differentiation. B cells also have innate abilities; they express several proteins of the TLR family, through which these cells recognize and respond to pathogen-associated ligands. TLR signals are important in T-independent and-dependent B cell responses (1–3). TLR stimulation of B cells enhances their Ag presentation capacity and promotes cytokine secretion, cell proliferation, and differentiation into Ab-secreting cells. TLR also regulate B cell localization and trafficking. TLR stimulation of the B1 B cell subpopulation facilitates their egress from the peritoneal cavity (4); marginal zone B cell location is also affected (5–7). TLR2/TLR9 stimulation triggers CD62L shedding in B cells, promoting accumulation in the spleen and decreased cell numbers in lymph nodes (8). TLR4-mediated B cell activation enhances homing to lymph nodes and localization to germinal centers (9).

Depending on whether they recognize pathogen membrane components or pathogen nucleic acids, TLR proteins are expressed on the cell surface or in endosomal compartments (10). All TLR except TLR3 signal through the adaptor protein MyD88; TLR3 and TLR4 signal via the adaptor protein Toll/IL-1R domain-containing adaptor-inducing IFN-β (TRIF) (10). The MyD88-dependent pathway leads to activation of MAPK and the transcription factors AP-1, IFN regulatory factor-5, and NF-κB, with subsequent production of proinflammatory cytokines. TRIF-mediated signaling results in IFN regulatory factor-3 transcription factor activation, type I IFN secretion, and NF-κB activation, which promotes proinflammatory cytokine expression. Although these signaling pathways are well studied, little is known of the molecular mechanisms that underlie TLR-mediated changes in cell behavior. Following pathogen challenge, dendritic cell (DC) migration decreases transiently and Ag capture increases (11). Both events required extensive actin cytoskeleton rearrangements that result in podosome disassembly and active endocytosis, for which MAPK activity is needed. Sequestration of the non–muscle motor protein myosin II by the class II MHC–associated invariant chain acts as a brake for DC motility after microbe detection (12). TLR signaling blocks monocyte and neutrophil chemotaxis; Rap1 GTPase and the MAPK ERK and p38 appear to be involved (13, 14).

In homeostatic conditions, B cells migrate continuously within the follicles of secondary lymphoid organs. CXCL13 chemokine signaling through its receptor CXCR5 supports B cell motility on the follicular stromal cell network, possibly assisted by adhesion molecules (15, 16). BCR signaling modulates chemokine-triggered B cell motility, and the molecular mechanisms involved in this process have begun to be defined (17). In the follicle, B cells might interact directly with pathogens or pathogen-derived ligands, which stimulates their TLR; TLR signaling effects on B cell behavior remain almost unknown. Lengthy in vitro exposure (18 h) of B cells to LPS leads to altered chemokine receptor expression, enhanced polarized cell morphology, and changes in cell velocity and direction (9). The signaling pathways involved in these processes remain undefined. The short-term effect of TLR ligands on cell dynamics has not been addressed.

In this study, we analyzed the regulation of B cell dynamics by TLR4 at different times. TLR4 is the receptor for LPS, an outer membrane component of Gram-negative bacteria, and is expressed in complex with MD2 at the B cell surface (3, 10); TLR4 function appears to be regulated by its homolog RP105, which also binds

Laboratorio de la Dinámica de las Células B, Departamento de Inmunología y Oncología, Centro Nacional de Biotecnología-Consejo Superior de Investigaciones Cientificas, Madrid E-28049, Spain

Received for publication June 19, 2013. Accepted for publication August 3, 2013.

L.B. is supported by a contract associated with Project Grant BFU2008-01194 from the Spanish Ministry of Economy and Competitiveness (MINECO). J.S.d.G. is supported by a contract from the Comunidad Autónoma de Madrid. This work was supported by grants from the European Union (Framework Programme 7–integrated project Masterswitch 223404 FP7) and Spanish MINECO (BFU2011-30097 to Y.R.C.).

L.B. designed parts of the study, performed the experiments, analyzed the data, and assisted in manuscript preparation. J.S.d.G. assisted in performing experiments, data analysis, and manuscript preparation. Y.R.C. designed and supervised all aspects of the project and wrote the manuscript.

Address correspondence and reprint requests to Dr. Yolanda R. Carrasco, Laboratorio de la Dinámica de las Células B, Departamento de Inmunología y Oncología, Centro Nacional de Biotecnología-Consejo Superior de Investigaciones Cientificas, Darwin 3, UAM-Campus Cantoblanco, Madrid E-28049, Spain. E-mail address ycarrasco@cnb.csic.es

The online version of this article contains supplemental material.

Abbreviations used in this article: BIRB, BIRB796; DC, dendritic cell; DIC, differential interference contrast; IRM, interference reflection microscopy; PD, PD184352; RT, room temperature; TRIF, Toll/IL-1R domain-containing adaptor-inducing IFN-β; WT, wild-type.

LPS (18, 19). We observed that TLR4 stimulation modulated B cell behavior in response to chemokines, although effects were not immediate; a minimum period of LPS exposure was necessary. We also found that the MyD88-dependent signaling pathway is needed, but ERK and p38 activity downstream of TLR4 appear not to be implicated. Rac GTPase activity was enhanced in TLR4-stimulated rather than in unstimulated B cells, and in response to CXCL13, Rac activity persisted longer in TLR4-stimulated B cells. These results help to clarify the mechanisms by which innate signals regulate B cell dynamics.

Materials and Methods

Mice and cells

Primary B cells were freshly isolated by negative selection (>95% purity) (17) from spleens of 3–5 mo-old wild-type (WT), MyD88-deficient [kindly provided by Dr. Carlos Ardavin, Centro Nacional de Biotecnología-Consejo Superior de Investigaciones Cientificas, Madrid, Spain (20)] and TRIF-deficient mice [kindly provided by Dr. Marina Freudenberg, Max-Planck-Institute of Immunobiology and Epigenetics, Freiburg, Germany (21)] on the C57BL/6 genetic background. For B cell purification, we used Dynabeads Mouse Pan-T isolation kit or, when indicated, Dynal Mouse B cell Negative Isolation kit (Dynal; Invitrogen). Animal experiments were approved by the Centro Nacional de Biotecnología-Consejo Superior de Investigaciones Cientificas Bioethics Committee and conform to institutional, national, and European Union regulations.

Purified B cells were used directly or cultured at 2×10^6/ml in RPMI 1640/10% FCS, alone or with LPS (2.5 μg/ml; from *Escherichia coli*, serotype 0182:B12; Sigma-Aldrich) for the times indicated. For time-lapse experiments, B cells were fluorescently labeled with CFSE or SNARF-1 probes (0.1 μM, 10 min, 37˚C; Molecular Probes) before use or in vitro culture. For chemical inhibitor treatments, B cells were cultured with inhibitor for 30 min before LPS was added; inhibitor was maintained in the medium during the LPS culture period. We used the MEK1 inhibitor PD184352 (PD; 0.2 μM), the MKK4/6 inhibitor BIRB796 (BIRB; 0.1 μM), both kindly provided by Dr. Ana Cuenda and made by custom synthesis (22), and the Rac inhibitor III EHop-016 (2.5 μM; Calbiochem/Millipore).

Time-lapse microscopy on planar lipid bilayers

Artificial planar lipid bilayers containing GPI-linked mouse ICAM-1 (density 150 molecules/μm^2) were prepared (17, 23). Planar membranes were assembled on FCS2 closed chambers (Bioptechs) and blocked with PBS/2% FCS (1 h, room temperature [RT]); immediately before use, they were coated with 100 nM recombinant murine CXCL13 or CCL21 (PeproTech). Immunofluorometric estimates of chemokine density on the membrane rendered a value of 30–40 molecules/μm^2. CFSE-labeled LPS-stimulated, and SNARF-1–labeled unstimulated B cells were mixed at a 1:1 ratio, injected into the warmed chamber (4×10^6; 37˚C), allowed to settle on the membranes (5–10 min), and imaging was initiated. Where indicated, B cells were treated with the specified chemical inhibitor during culture. Confocal fluorescence, differential interference contrast (DIC), and interference reflection microscopy (IRM) images were acquired every 8 s for 15 min; two or three consecutive videos were acquired in different positions at the membranes. We performed the assays in PBS/0.5% FCS/0.5 g/l D-glucose/2 mM $MgCl_2$/0.5 mM $CaCl_2$; when indicated, LPS (2.5 μg/ml) was present in the medium. Images were acquired on an Axiovert LSM 510-META inverted microscope with a 40× oil immersion objective (Zeiss). Imaging analysis of cell dynamic parameters and other quantitative measurements were done using Imaris 7.0 software (Bitplane) and ImageJ software (National Institutes of Health).

Western blot

Freshly isolated primary B cells (5×10^6) were cultured in depletion medium (RPMI 1640/0.5% FCS; 1 h, 37˚C) and then stimulated with LPS (2.5 μg/ml; with shaking) for the times specified; when indicated, B cells were treated with inhibitors for the last 30 min of depletion culture. For CXCL13/CXCR5 signaling studies, B cells (5×10^6) were cultured in depletion medium (1 h), LPS was added, and cells were further incubated (4 h); cells were collected, washed, and stimulated with CXCL13 (100 nM; with shaking) in depletion medium (0.5 ml) for the indicated times. Ice-cold PBS was added and B cells centrifuged (2,000 rpm, 5 min, 4˚C) and lysed in lysis buffer (50 mM Tris-HCl [pH 7.5], 150 mM NaCl, 1 mM EDTA, 1% Triton X-100) with protease and phosphatase inhibitors (Roche; 30 min, 4˚C). Lysates were centrifuged (14,000 rpm, 30 min, 4˚C) and supernatants collected and stored at −80˚C. B cells cultured in RPMI 1640/10% FCS alone or with LPS (4 h) were lysed in RIPA lysis buffer as above and used to evaluate Rho GTPases and WAVE-2 protein levels. Total protein was quantified with the Micro BCA Protein assay kit (Thermo Scientific), separated by SDS-PAGE, and transferred to polyvinylidene difluoride membranes (Bio-Rad). Blots were blocked with 2% BSA in TBST (10 mM Tris-HCL [pH 8], 150 mM NaCl, and 0.1% Tween-20) (1 h, RT) and incubated with rabbit Abs anti-ERK1/2, –phospho-ERK1/2 (Thr^{202}/Tyr^{204}), –phospho-p38 (Thr^{180}/Tyr^{182}; 12F8), –WAVE-2 (D2C8) (Cell Signaling Technology), -Cdc42 (ACD03-A), -Rac123 (from G-LISA kit BK125; Cytoskeleton), -p38α (C-20; Santa Cruz Biotechnology), -RhoA/B/C (07-1463; Upstate Biotechnology, Millipore), or mouse anti–α-tubulin (clone DM1A; Sigma-Aldrich) (overnight, 4˚C), followed by HRP-conjugated secondary Abs (DakoCytomation; 1 h, RT). The signal was detected with the ECL detection system (GE Healthcare). Signal intensity values in arbitrary units were quantified for each protein using ImageJ software (National Institutes of Health) and normalized to the tubulin signal; p-ERK1/2 and p-p38 levels were divided by ERK1/2 and p38 levels, respectively, at each time point and relative to time 0.

Immunofluorescence

LPS-treated and untreated B cells were in contact with membranes containing GPI-linked ICAM-1 and CXCL13 coating (30 min), fixed with 4% paraformaldehyde (10 min, 37˚C), permeabilized with PBS/0.1% Triton X-100 (5 min, RT), blocked with PBS/2% FCS/2% BSA (overnight, 4˚C), and stained with Alexa Fluor-647 phalloidin (Molecular Probes) and rabbit anti-WAVE-2 (Cell Signaling Technology) plus Alexa Fluor-488 goat anti-rabbit IgG (Southern Biotechnology Associates) (30 min, RT). FCS2 chambers were imaged by confocal fluorescent microscopy on the Zeiss Axiovert inverted microscope (Zeiss).

Rho GTPase activation assays

Rho GTPase activity was determined in B cell lysates using the G-LISA Rac activation (BK125), G-LISA Cdc42 Activation (BK127), and G-LISA RhoA activation assay kits (BK124; Cytoskeleton). B cells were stimulated as for CXCL13/CXCR5 signaling studies by Western blot. Ice-cold PBS was added and B cells centrifuged (2000 rpm, 5 min, 4˚C); lysis and GTPase activity measurement was done following G-LISA kit instructions.

Flow cytometry

B cells were stained with FITC-conjugated rat anti-mouse CD69 and PE-rat anti-mouse CD86 (BD Biosciences; 30 min, 4˚C). To measure F-actin content, B cells were fixed with 2% paraformaldehyde (10 min, RT), permeabilized with PBS/0.2% saponin (5 min, RT), and stained with Alexa Fluor-647 phalloidin (Molecular Probes; 20 min, RT). Samples were analyzed in an FACSCalibur cytometer (BD Biosciences). To quantify the *x*-fold increase in CXCR5 and F-actin levels, we calculated the ratio between the mean fluorescence value of interest (4-h LPS-treated, 4-h untreated) and that of the control condition (freshly isolated B cells) in each experiment.

Statistical analysis

Graphs and statistical analysis were done using Prism 4.0 software (GraphPad). Two-tailed unpaired Student *t* test was applied to compare each condition with its control; $*p < 0.05$, $**p < 0.001$, $***p < 0.0001$.

Results

Short-term TLR4 stimulation modifies B cell behavior

We analyzed chemokine-triggered B cell dynamics alone or in the presence of the TLR4 ligand LPS. To study the behavior of primary B cells isolated from WT mouse spleen, we used a two-dimensional model based on artificial planar lipid bilayers combined with real-time confocal fluorescence microscopy (17). This two-dimensional model allowed us to mimic the in vivo dynamic parameters of B cells described using multiphoton microscopy and study primary B cell behavior in response to stimuli. The artificial membranes contained ICAM-1 (150 molecules/μm^2), the ligand of the integrin LFA-1, anchored by GPI, to promote B cell adhesion and migration in response to the membrane CXCL13 coating (40 molecules/μm^2). CFSE-labeled B cells were allowed to settle on the membranes, alone or with LPS (2.5 μg/ml), and cell behavior was monitored for up to 1 h. This LPS dose promoted B cell activation (evaluated as CD69 and CD86 upregulation; Fig. 1A). The frequencies of cells showing membrane protrusion activity

(cell polarization, estimated by DIC) and cell migration (motile cells, estimated by DIC and IRM) in response to CXCL13 were nearly unmodified by LPS stimulation (Fig. 1B). We observed no changes in motile B cell mean velocity, directionality (measured as straightness index), or track (Fig. 1C, 1D, Supplemental Video 1). TLR4 stimulation thus had no effect on CXCL13-driven B cell behavior at the times analyzed.

Cell dynamics were modified when we prestimulated B cells with LPS for a short period (4 h); at this time, B cells showed signs of activation ($CD69^+$; Fig. 1E). TLR4 stimulation increased B cell polarization and enhanced both polarization and migration in response to CXCL13 (Fig. 1F, Supplemental Video 2). Whereas mean velocity was unchanged, cell directionality increased significantly in LPS-treated B cells (Fig. 1G, 1H, Supplemental Video 2). B cell contact areas with the membranes, mediated by LFA-1/ICAM-1 interactions and detected by IRM, were smaller when stimulated by TLR4 (Fig. 2A, 2B). Contact signal intensity was lower in LPS-treated than in untreated B cells (Fig. 2B), suggesting weaker LFA-1–mediated adhesion to the membrane. Polarization, migration, and mean speed increased in 24-h–cultured, unstimulated B cells, possibly promoted by TLR/receptor detection of cell death; at this time point, TLR4 stimulation yielded no differences in cell behavior compared with unstimulated cells (Supplemental Fig. 1, Supplemental Video 3). To determine whether short-term TLR4 signaling modified the B cell response to other chemokines, we performed similar experiments using CCL21 to coat the artificial membrane. In response to CCL21, cell polarization and migration frequencies were significantly higher in 4-h LPS–treated than in untreated B cells (Fig. 2C); mean velocity and cell directionality index values were similar for both (Fig. 2D). B cell mean velocity values in response to CCL21 were slightly but significantly ($p < 0.05$) lower than in response to CXCL13.

The B cell pool isolated from spleen had contaminants of $CD11b^+$ cells (monocytes/macrophages, DC; ~5%) (Supplemental Fig. 2A), potent cytokine producers when stimulated with LPS. To verify that the regulation of cell dynamics was a direct effect of TLR4 signaling on B cells, we purified them using a different

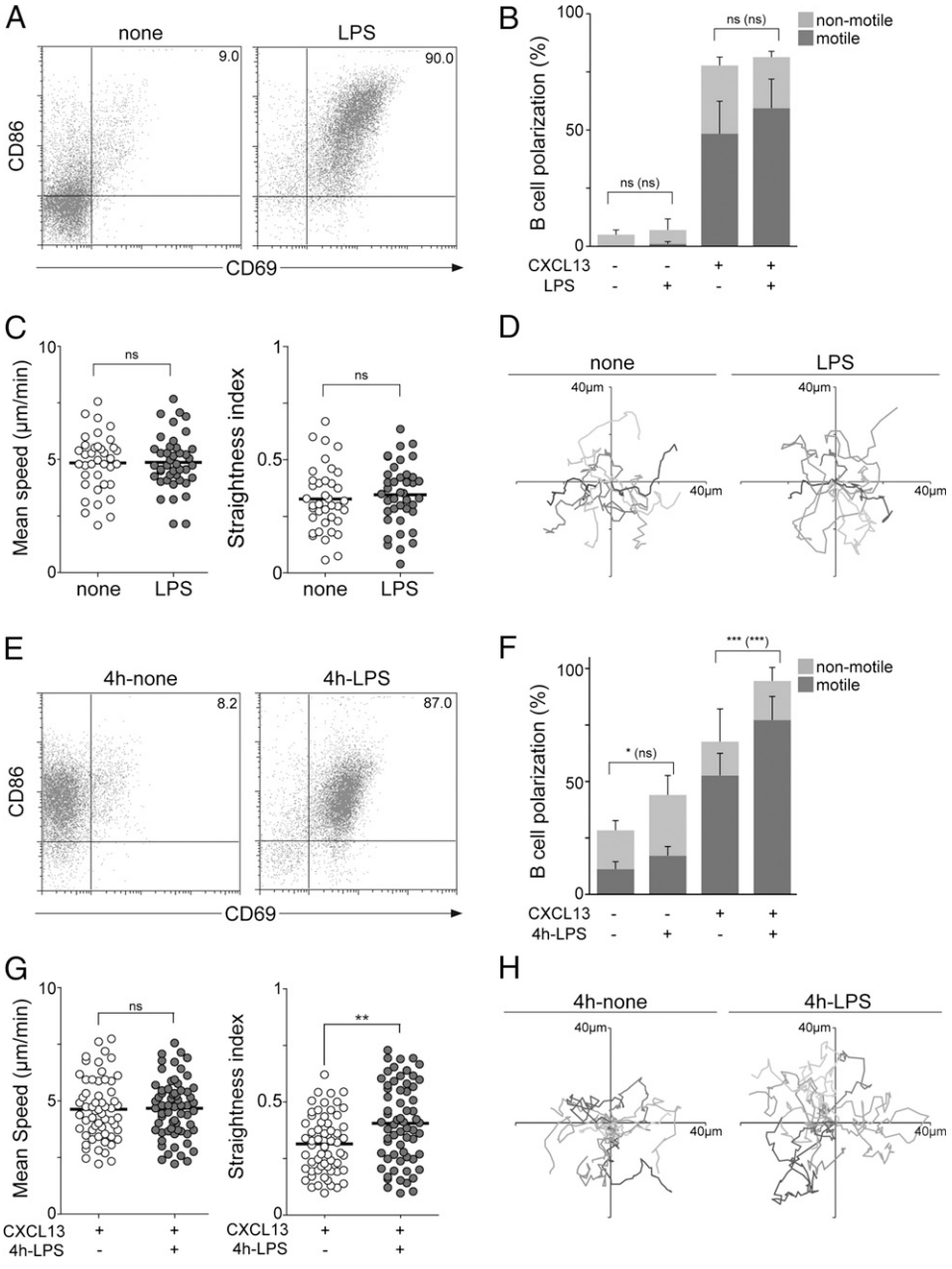

FIGURE 1. TLR4-mediated effects on B cell dynamics. (**A**) Representative CD86 and CD69 flow cytometry profiles of primary B cells cultured alone (none; *left panel*) or with LPS (*right panel*) for 20 h. (**B**) Cell polarization frequencies of B cells settled on ICAM-1–containing membranes, uncoated or CXCL13-coated, alone or with LPS; nonmotile and motile B cell fractions are shown for each condition. Mean speed and straightness index values (**C**) and representative tracks (**D**) ($n = 10$) of B cells migrating on ICAM-1/CXCL13 membranes alone (none) or with LPS. (**E**) Representative CD86 and CD69 flow cytometry profiles of primary B cells cultured alone (none; *left panel*) or with LPS (*right panel*) for 4 h. (**F**) Cell polarization frequencies of B cells, unstimulated or stimulated with LPS (4h-LPS), and then settled on ICAM-1–containing membranes, uncoated, or CXCL13 coated; nonmotile and motile B cell fractions are shown for each condition. Mean speed and straightness index values (**G**) and representative tracks (**H**) ($n = 10$) of motile B cells in (F). Data in (B) are the mean ± SD ($n = 3$ experiments); data in (F) are the mean ± SD of three representative experiments ($n = 12$); data in (C) and (G) are derived from three experiments, respectively, where each dot corresponds to a single cell. Statistic significance evaluated by Student *t* test for polarization and motile cells (in parentheses); mean speed and straightness is shown in each case. $*p < 0.05$, $**p < 0.001$, $***p < 0.0001$.

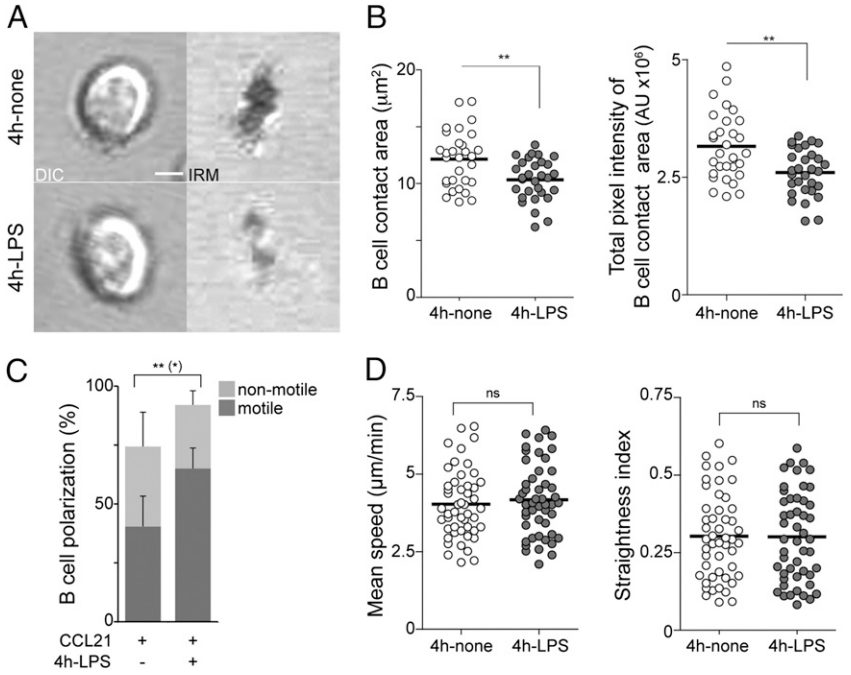

FIGURE 2. LPS stimulation modifies B cell adhesion to ICAM-1–containing membranes and enhances the B cell response to CCL21. (**A**) DIC and IRM images of representative B cells, unstimulated (4h-none) or stimulated with LPS (4h-LPS), and then settled on ICAM-1/CXCL13 membranes. Scale bar, 2 μm. (**B**) Contact area with the membrane (in μm^2; *left panel*) and total pixel intensity of the contact area (signal intensity in arbitrary units [AU]; *right panel*), detected by IRM, in unstimulated (4h-none) and LPS-stimulated (4h-LPS) B cells settled on ICAM-1/CXCL13 membranes. (**C**) Cell-polarization frequencies, indicating fraction of nonmotile and motile cells, for unstimulated and LPS-stimulated (4h-LPS) B cells settled on ICAM-1/CCL21 membranes. (**D**) Mean speed and straightness index values for motile B cells in (C). Data in (B) correspond to a representative experiment ($n = 3$); values in (C) are mean ± SD ($n = 4$ experiments), and in (D), data are derived from three experiments; each dot in (B) and (D) corresponds to a single cell. Statistic significance evaluated by Student *t* test for polarization and motile cells (in parentheses); mean speed and straightness is shown in each case. $*p < 0.05$, $**p < 0.001$.

approach; we diminished five times the presence of $CD11b^+$ cells (Supplemental Fig. 2A). The exposure of CD11b-depleted B cells to LPS for 4 h had the same effects on cell activation and dynamics as in B cells not depleted for $CD11b^+$ cells (Supplemental Fig. 2B–D). These data altogether suggest that TLR4 stimulation primes B cells to enhance their response to CXCL13 and CCL21.

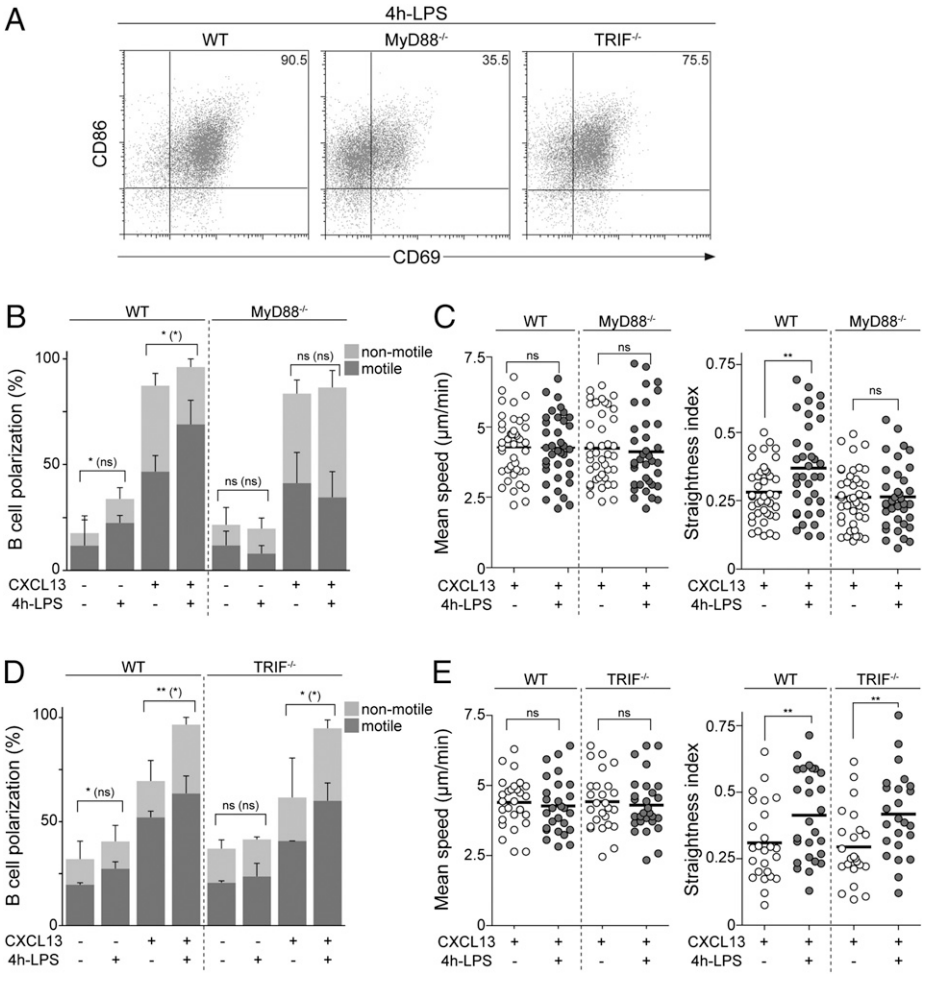

FIGURE 3. MyD88 but not TRIF is needed for TLR4-mediated effects on B cell dynamics. (**A**) Representative CD86 and CD69 flow cytometry profiles of WT, $MyD88^{-/-}$ and $TRIF^{-/-}$ B cells cultured with LPS (4 h). (**B**) Cell polarization frequencies of WT and $MyD88^{-/-}$ B cells, unstimulated or stimulated with LPS (4h-LPS), and then settled on ICAM-1–containing membranes, uncoated or CXCL13 coated; nonmotile and motile cell fractions are shown for each condition. (**C**) Mean speed and straightness index values of motile WT and $MyD88^{-/-}$ B cells in (B) on ICAM-1/CXCL13 membranes. (**D**) As in (B), for WT and $TRIF^{-/-}$ B cells. (**E**) Mean speed and straightness index values of motile WT and $TRIF^{-/-}$ B cells in (D) on ICAM-1/CXCL13 membranes. Values in (B) are the mean ± SD of three representative experiments ($n = 12$) for WT B cells and the mean ± SD ($n = 3$) for $MyD88^{-/-}$ B cells; in (C) are derived from three experiments; data in (D) are the mean ± SD of three representative experiments ($n = 12$) for WT B cells, and the mean ± SD ($n = 2$) for $TRIF^{-/-}$ B cells; in (E) are derived from two experiments; each dot in (C) and (E) corresponds to a single cell. Statistic significance evaluated by Student *t* test for polarization and motile cells (in parentheses); mean speed and straightness is shown in each case. $*p < 0.05$, $**p < 0.001$.

TLR4 effects on B cell dynamics depend on the MyD88 signaling pathway

TLR4 can signal via two routes, the MyD88- and the TRIF-dependent pathways. Using B cells isolated from MyD88- or TRIF-deficient mouse spleens, we studied which of these signaling cascades was responsible for the effects on B cell behavior. MyD88$^{-/-}$ B cells expressed very little surface CD69 after short-term (4 h) LPS stimulation, a difference from TRIF$^{-/-}$ B cells, for which CD69 levels were similar to those of WT B cells (Fig. 3A). We cultured fluorescently labeled MyD88$^{-/-}$, TRIF$^{-/-}$, and WT B cells, alone or with LPS (4 h), then mixed CFSE-labeled MyD88$^{-/-}$ or TRIF$^{-/-}$ B cells at a 1:1 ratio with SNARF-1–labeled WT B cells, allowed them to settle on membranes containing GPI–ICAM-1 alone or with CXCL13 coating (ICAM-1/CXCL13 membranes), and monitored cell behavior by real-time microscopy. WT B cells behaved as described (Fig. 3B, 3C). Cell polarization did not increase in LPS-stimulated MyD88$^{-/-}$ B cells, nor did exposure to CXCL13 enhance polarization, migration, or directionality of these cells; mean speed values were unaffected (Fig. 3B, 3C, Supplemental Video 4). In contrast, in LPS-stimulated TRIF$^{-/-}$ B cells, these dynamic parameters were modified nearly as for LPS-treated WT B cells (Fig. 3D, 3E, Supplemental Video 5). The results indicated that TLR4-triggered changes in chemokine-mediated B cell behavior are dependent on the MyD88 signaling pathway and independent of TRIF-mediated signals.

ERK and p38 activation downstream of TLR4 are not necessary for LPS modulation of B cell dynamics

To determine which MyD88-dependent pathway signaling molecules are implicated in TLR4-mediated modulation of B cell behavior, we studied the role of ERK1/2 and p38. Both of these MAPK have important functions in TLR signaling in immune cells (10), as well as in cell migration (24). To analyze ERK and p38 activation by LPS stimulation of TLR4 in B cells, we detected p-ERK1/2 and p-p38 in Western blot. TLR4 stimulation activated

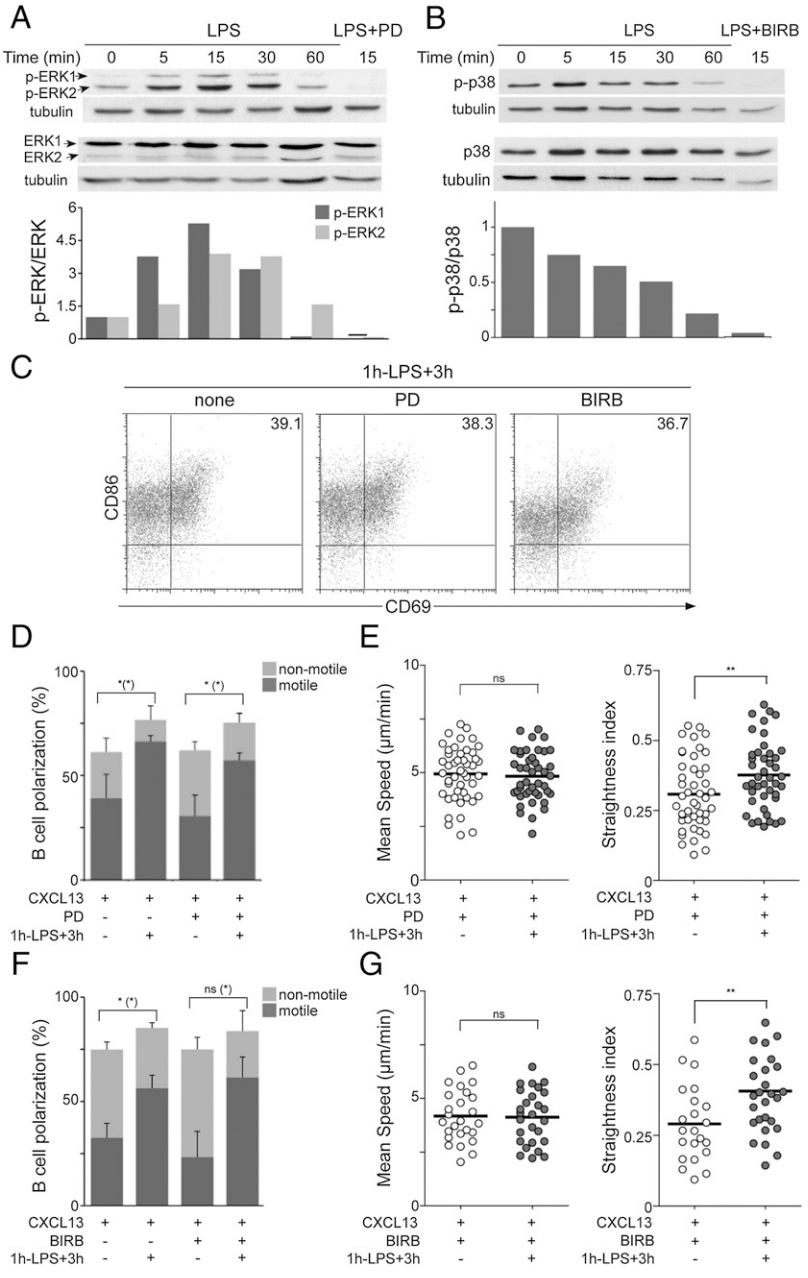

FIGURE 4. ERK and p38 activities downstream of TLR4 are not needed for modification of B cell dynamics. (**A**) Western blot showing ERK1/2 (ERK) and phosphorylated ERK1/2 (p-ERK) levels, before and after LPS stimulation, in B cells untreated (LPS) or treated with the inhibitor PD (LPS+PD); tubulin was used as loading control. Quantification of p-ERK1 and p-ERK2 levels at each time point compared with time 0 (*bottom panel*; see *Materials and Methods* for details). (**B**) p38α (p38) and p-p38 levels in B cells untreated (LPS) or treated with the inhibitor BIRB (LPS+BIRB), as in (A). Quantification of p-p38 levels at each time point compared with time 0 (*bottom panel*). (**C**–**G**) B cells were untreated or treated with inhibitors (PD, BIRB; 30 min, 37°C), stimulated with LPS alone or in the presence of the inhibitors (1 h, 37°C), washed, and cultured (3 h); B cells were then analyzed by flow cytometry or settled on ICAM-1/CXCL13 membranes for cell-dynamics studies. (C) Representative CD86 and CD69 flow cytometry profiles of B cells cultured as specified above. Frequencies of B cell polarization, indicating fractions of nonmotile and motile cells (D) and mean speed and straightness index values (E) for motile B cells in each PD treatment condition. B cell polarization frequencies, indicating fractions of nonmotile and motile cells (F) and mean speed and straightness index values (G) for motile B cells in each BIRB treatment condition. Data in (A) and (B) show one representative experiment of three performed; values in (D) and (F) are mean ± SD ($n = 3$) and in (E) and (G) are derived from one representative experiment ($n = 3$); each dot corresponds to a single cell. Statistic significance evaluated by Student t test for polarization and motile cells (in parentheses); mean speed and straightness is shown in each case. $*p < 0.05$, $**p < 0.001$.

ERK1/2, with a maximum at 15 min, and returned to basal levels at 1 h (Fig. 4A). In contrast, p38 was not activated, but was gradually dephosphorylated after TLR4 stimulation; we found high basal p-p38 levels (time 0) in B cells (Fig. 4B).

We impaired ERK activation with the chemical inhibitor PD, which blocks the activity of MEK1 (an upstream activator of ERK); pretreatment of B cells with 0.2 μM PD blocked TLR4-induced ERK activation (Fig. 4A). For cell dynamics assays in the two-dimensional model, we pretreated B cells with PD (30 min), added LPS (1 h), eliminated PD and LPS from the medium, and further incubated the B cells (3 h) before assay. This LPS stimulation protocol (1 h LPS + 3 h) promoted increases in cell polarization and migration similar to those after 4-h LPS treatment (Supplemental Fig. 3) and allowed inhibitor removal to minimize interference with ERK activation by the chemokine receptor (Fig. 4D). In short (1-h) and longer (4-h) protocols, PD treatment did not alter CD86 and CD69 expression by LPS-stimulated B cells (Fig. 4C and not shown). PD-treated and untreated B cells labeled with distinct probes (CFSE, SNARF-1) were mixed at a 1:1 ratio and settled on ICAM-1/CXCL13 membranes; PD treatment caused no alterations in cell behavior parameters (Fig. 4D, 4E). After LPS stimulation, PD-treated B cells showed polarization and migration frequencies, as well as mean speed and directionality index values similar to those of untreated cells (Fig. 4D, 4E). These data suggest that ERK activation by TLR4 is not involved in the regulation of B cell behavior.

To analyze the contribution of p38 activity, we used the specific chemical inhibitor BIRB, which blocks all p38 isoforms. Pretreatment of B cells with 0.1 μM BIRB reduced p-p38 levels in TLR4-stimulated B cells (Fig. 4B) without altering CD86 and CD69 expression (Fig. 4C and not shown). BIRB treatment did not modify the behavior of B cells in contact with ICAM-1/CXCL13 membranes (Fig. 4F, 4G), nor did it interfere with LPS-mediated enhancement of cell polarization, migration, or directionality (Fig. 4F, 4G). These findings indicate that p38 activity is not needed for TLR4-mediated effects on B cell dynamics.

TLR4 stimulation increases CXCL13-triggered ERK1/2 activation in B cells

To further characterize the molecular mechanisms that control TLR4-mediated effects on B cell dynamics, we analyzed signaling downstream of the CXCL13 receptor CXCR5. We observed that 4-h LPS stimulation promoted a slight but significant increase in CXCR5 levels on the B cell surface (Fig. 5A). We studied ERK1/2 and p38 activation by CXCL13 stimulation in 4-h LPS–treated and untreated B cells; MAPK activation was evaluated as before. TLR4 stimulation did not alter total ERK1/2 or p-ERK levels in B cells (Fig. 5B). In response to CXCL13 stimulation, p-ERK levels were nonetheless significantly higher in 4-h LPS–treated than in untreated B cells at all times analyzed (Fig. 5B). There were no differences in p-p38 or p38 protein levels between 4-h LPS–treated and untreated B cells before and after CXCR5 stimulation (Fig. 5C). We detected no p38 activation after CXCR5 stimulation, only dephosphorylation (Fig. 5C). TLR4-induced effects on B cell dynamics might thus be mediated by enhanced ERK1/2 activation downstream of CXCR5, assisted by the slight increase in surface CXCR5 levels.

Rac GTPase activity is high and persistent in LPS-stimulated B cells

In response to distinct stimuli, the members of the Rho subfamily of GTPases, namely Rho, Rac, and Cdc42, regulate actin cytoskeleton rearrangement, cell polarization, and migration (25, 26). We investigated the implication of Rho GTPases in the TLR4-mediated

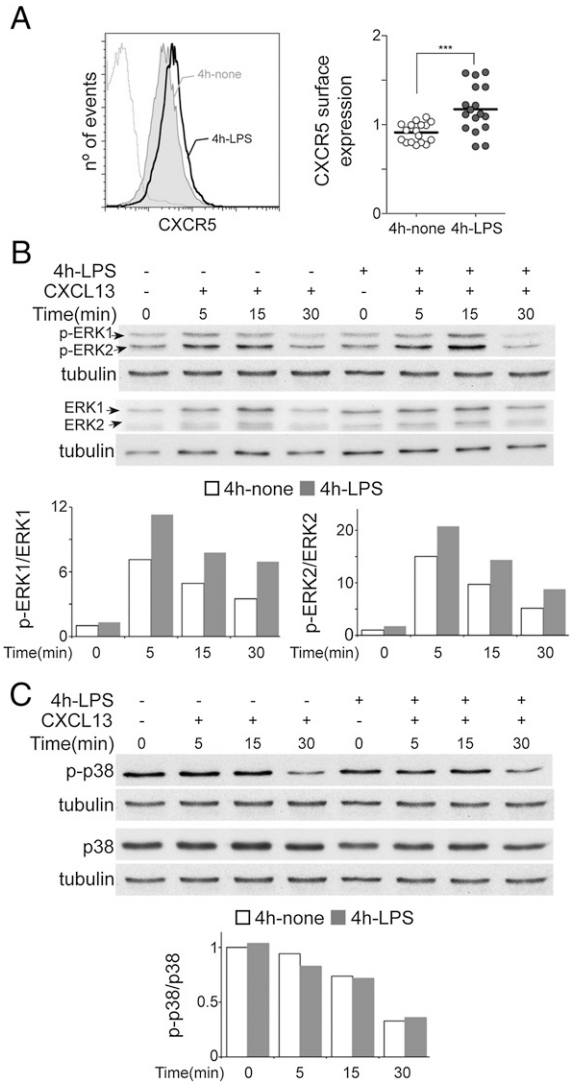

FIGURE 5. LPS-stimulated B cells have increased ERK activation after CXCL13 signaling. (**A**) Representative CXCR5 profiles of B cells unstimulated (4h-none) or stimulated with LPS (4h-LPS) (*left panel*); quantification of variation in CXCR5 levels in 4h-none and 4h-LPS B cells, relative to freshly isolated B cells (*right panel*) (see *Materials and Methods*); each dot is a single experiment. (**B**) Western blot showing ERK1/2 (ERK) and phosphorylated ERK1/2 (p-ERK) levels before and after CXCL13 stimulation, in B cells cultured in depletion medium (4 h) alone or with LPS (4h-LPS); tubulin was used as loading control. Quantification of p-ERK1 and p-ERK2 levels at each time point compared with time 0 for unstimulated B cells (*bottom panel*; see *Materials and Methods*). (**C**) p38α (p38) and p-p38 in B cells as in (B); p-p38 levels were quantified as in (B). (B) and (C) show one representative experiment of three performed. ***$p < 0.0001$.

effects on B cell behavior. We studied levels and activity of these proteins in LPS-treated compared with untreated B cells. Rho, Rac, and Cdc42 protein levels were not altered by TLR4 stimulation (Fig. 6A). We measured activation (GTP-bound form) in B cell lysates using G-LISA techniques (see *Materials and Methods*) and found no differences in RhoA and Cdc42 activities between 4-h LPS–treated and untreated B cells in basal conditions (time 0) or after CXCR5 stimulation (Fig. 6B). Rac activity was nonetheless significantly higher in TLR4-stimulated than in unstimulated B cells; CXCR5-triggered Rac activity was also enhanced and sustained in TLR4-stimulated B cells (Fig. 6B).

Rac promotes actin polymerization at nascent cell protrusions (26). We measured the amount of polymerized actin (F-actin) per

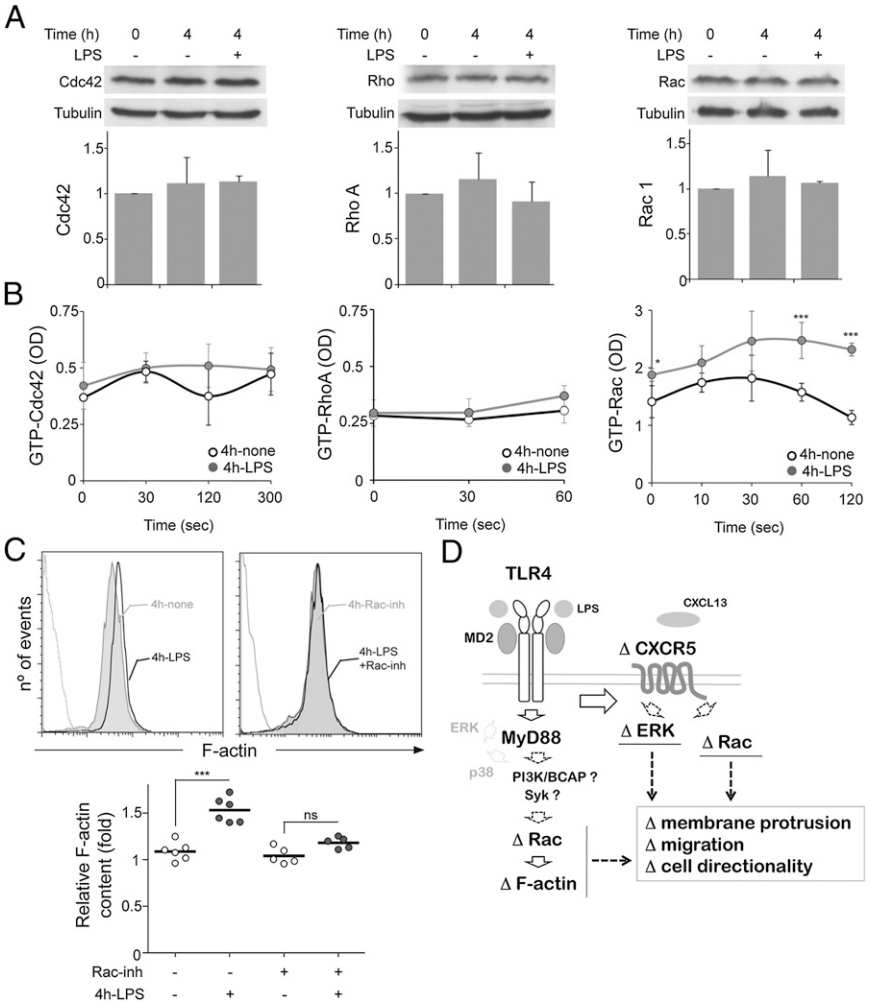

FIGURE 6. TLR4 signaling increases Rac GTPase activity. (**A**) Cdc42, RhoA/B/C (Rho), and Rac123 (Rac) protein levels in freshly isolated B cells (time 0) or after culture (4 h), alone or with LPS; tubulin was used as loading control. Quantification of Rho GTPase levels in each condition compared with freshly isolated B cells (time 0; *bottom panel*); data show mean ± SD ($n = 3$ experiments). (**B**) B cells cultured in depletion medium (1 h) were unstimulated (4h-none) or stimulated with LPS (4h-LPS) (4 h, 37˚C) and then stimulated with CXCL13 as indicated, lysed, and evaluated for Cdc42 (*left panel*), RhoA (*center panel*), and Rac123 (Rac; *right panel*) GTPase activity using G-LISA (see *Materials and Methods*); data show mean ± SD ($n = 3$ experiments). (**C**) Representative F-actin profiles of B cells unstimulated or LPS-stimulated (4h-LPS), untreated (*left panel*) or treated (*right panel*) with the Rac inhibitor III (Rac-inh). Variation in B cell F-actin levels for each condition relative to freshly isolated B cells (*bottom panel*); each dot is a single experiment. (**D**) Scheme of the signaling pathways implicated in TLR4-mediated effects on B cell dynamics. ***$p < 0.0001$. BCAP, B cell adapter for PI3K.

cell by flow cytometry and found significantly higher F-actin levels in 4-h LPS–treated than in untreated B cells (Fig. 6C). F-actin levels did not increase in 4-h LPS–treated B cells incubated with the Rac inhibitor III EHop-016 (2.5 μM; see *Materials and Methods*) (Fig. 6C), indicating that Rac activity was responsible for the enhanced actin polymerization. WAVE-2, a member of the Wiskott-Aldrich syndrome protein family, is a Rac effector involved in actin polymerization and cell protrusion (27). Using immunofluorescence and confocal microscopy, we found that WAVE-2 accumulated close to F-actin–rich areas of the B cell contact plane with the membrane in 4-h LPS–treated and untreated B cells (Supplemental Fig. 4A). Although WAVE-2 levels remain unchanged by LPS treatment (Supplemental Fig. 4B), its localization at cell protrusions suggested that WAVE-2 assisted Rac functions in B cells. The data thus point to Rac as a major effector of TLR4 to modify B cell dynamics.

Discussion

Regulation of B cell behavior and location in secondary lymphoid organs is critical for efficient B cell function and response; chemokines and Ag have important roles in this process. In this study, we show that B cell exposure to the pathogen-derived ligand LPS modifies cell dynamics over time. LPS/TLR4 signaling leads to increased B cell polarization, migration, and directionality in response to CXCL13; MyD88 and Rac GTPases are involved in these changes. We propose that B cell pathogen sensing by innate receptors such as TLR4 shapes cell dynamics, thus improving B cell Ag-seeking efficiency in the follicle.

We found that at doses that activate B cells, a minimum period of LPS exposure (1-h LPS + 3-h or 4-h LPS) was needed to provoke detectable changes in chemokine-triggered B cell behavior. With a tiny presence (~1%) in the in vitro culture of $CD11b^+$ cell contaminants (macrophages/DCs; potent cytokine producers when LPS stimulated), LPS exposure had the same effects on B cells. Although we cannot completely discard an indirect effect of the small fraction of $CD11b^+$ cells on B cell dynamics in presence of LPS, the modulation of B cell dynamics appears to be mediated by direct TLR4 stimulation of B cells. TLR4 might act at the gene expression level to regulate B cell dynamics. Long-term TLR4 stimulation (18 h) increased Gnai2 and decreased Rgs1 gene expression, promoting strong chemotactic responses in B cells (9). These results differ from data in monocytes and DC, in which LPS exposure promotes firmed adhesion and blocks chemokine-mediated cell polarization within minutes (11, 14). Although the LPS dose and/or LPS origin could explain in part these differences, we propose that the distinct function and LPS sensitivity of B cells compared with monocytes or DC support the different cell responses.

TLR4 signals through MyD88- and TRIF-dependent pathways. We show that MyD88, but not TRIF, is needed for the LPS-mediated effects on B cell dynamics. Other reports implicated MyD88-independent pathways in TLR4-induced modifications in cell dynamics and actin cytoskeleton in DC and macrophages (11, 28). The MyD88 pathway activates ERK and p38 (10); our data using chemical inhibitors suggested that these MyD88 targets are not implicated in modulation of B cell dynamics. A recent report

links TLR signaling with PI3K activation through B cell adapter for PI3K, which also interacts with MyD88 (29). PI3K has central roles in cell survival and proliferation, as well as in cell adhesion and migration (30). In addition, TLR9 signaling leads to Syk activation via the MyD88 pathway in B cells (31). Syk is involved in integrin activation and cell migration downstream of chemokine receptors and the BCR (32, 33). Further studies are needed to address the roles of PI3K and Syk in the modulation of B cell dynamics by TLR signaling. Finally, the detection of certain CD69 upregulation in LPS-exposed MyD88$^{-/-}$ B cells (Fig. 3A) might be due either to the composition of the LPS used, that it could activate other pattern-recognition receptors (34), or to the activation of alternative routes downstream TLR4 that target NF-κB activation (29, 35); although the TRIF pathway activates NF-κB, another attractive possibility is that PI3K is involved in a MyD88-independent manner.

ERK and/or p38 have opposite roles in regulating neutrophil migration in response to fMLF (36). Whereas ERK enhances GRK2-mediated chemokine receptor desensitization and thus inhibits cell migration, p38 blocks GRK2 activity and thus promotes migration. Via a p38-dependent pathway, the TNF-α inflammatory signal promotes firm cell adhesion and impairs IL-8–mediated neutrophil migration (13). The equilibrium between ERK and p38 activities dictates neutrophil dynamics, with each of these MAPK regulated by distinct inflammatory signals. In DC, the combined inhibition of p38 and ERK downstream of TLR4 signaling impeded podosome disassembly, suggesting a role for both MAPK in the transient arrest of DC migration after LPS stimulation (11). Our data using chemical inhibitors in B cells suggested that TLR4 activation of ERK and p38 is not involved in the LPS-mediated modulation of B cell dynamics. We nonetheless found that CXCL13 stimulation increased ERK activation in LPS-treated compared with untreated B cells, with no change in p38 activity; this new balance of ERK/p38 activities might be linked to the behavior changes observed in TLR4-stimulated B cells. The slight increase in cell-surface CXCR5 levels might increase ERK activation without altering p38 activity. More studies need to be done to confirm the consequences of these observations in CXCL13-triggered B cell behavior.

Short-term TLR4 stimulation of B cells clearly changes Rac GTPase activity, but not RhoA or Cdc42. Rac activity is higher in LPS-stimulated than in unstimulated B cells, leading to increased F-actin levels in the former. Further, Rac activation by CXCL13/CXCR5 signaling is persistent in LPS-stimulated B cells. These Rac features might be responsible for enhanced membrane protrusion activity. Rac thus appears to be an important downstream effector of TLR4 in the regulation of B cell behavior. Rac has also a role in DC behavior after TLR4-mediated maturation (37). Rac GTPases control a variety of cytoskeletal molecules and are involved in cell polarization, migration, and adhesion (25, 26). With the motor protein myosin, which controls actin-based contractility, Rac has been implicated in the control of cell directionality in nonimmune cells (38). The association of Rac with the LPS-induced increase in B cell directionality requires further study. We propose a model (Fig. 6D) in which TLR4 detection of pathogen ligands triggers a signaling cascade via MyD88, possibly involving PI3K and/or Syk activation, that leads to increased Rac activation in B cells. Rac activity promotes actin cytoskeleton rearrangements that boost B cell responses to chemokines. The increased CXCL13-triggered ERK activation, possibly related with the increase in CXCR5 levels at surface, and persistent Rac activity in TLR4-stimulated B cells will assist the enhanced response to CXCL13. By shaping cell behavior, TLR4 signaling might improve B cell function.

Acknowledgments

We thank I. Antón, A. Cuenda, M. Mellado, and S. Minguet for critical reading of the manuscript and C. Mark for editorial assistance.

Disclosures

The authors have no financial conflicts of interest.

References

1. Pasare, C., and R. Medzhitov. 2005. Control of B-cell responses by Toll-like receptors. *Nature* 438: 364–368.
2. Hou, B., P. Saudan, G. Ott, M. L. Wheeler, M. Ji, L. Kuzmich, L. M. Lee, R. L. Coffman, M. F. Bachmann, and A. L. DeFranco. 2011. Selective utilization of Toll-like receptor and MyD88 signaling in B cells for enhancement of the antiviral germinal center response. *Immunity* 34: 375–384.
3. Rawlings, D. J., M. A. Schwartz, S. W. Jackson, and A. Meyer-Bahlburg. 2012. Integration of B cell responses through Toll-like receptors and antigen receptors. *Nat. Rev. Immunol.* 12: 282–294.
4. Ha, S. A., M. Tsuji, K. Suzuki, B. Meek, N. Yasuda, T. Kaisho, and S. Fagarasan. 2006. Regulation of B1 cell migration by signals through Toll-like receptors. *J. Exp. Med.* 203: 2541–2550.
5. Groeneveld, P. H., T. Erich, and G. Kraal. 1985. In vivo effects of LPS on B lymphocyte subpopulations. Migration of marginal zone-lymphocytes and IgD-blast formation in the mouse spleen. *Immunobiology* 170: 402–411.
6. Rubtsov, A. V., C. L. Swanson, S. Troy, P. Strauch, R. Pelanda, and R. M. Torres. 2008. TLR agonists promote marginal zone B cell activation and facilitate T-dependent IgM responses. *J. Immunol.* 180: 3882–3888.
7. Cinamon, G., M. A. Zachariah, O. M. Lam, F. W. Foss, Jr., and J. G. Cyster. 2008. Follicular shuttling of marginal zone B cells facilitates antigen transport. *Nat. Immunol.* 9: 54–62.
8. Morrison, V. L., T. A. Barr, S. Brown, and D. Gray. 2010. TLR-mediated loss of CD62L focuses B cell traffic to the spleen during *Salmonella typhimurium* infection. *J. Immunol.* 185: 2737–2746.
9. Hwang, I. Y., C. Park, K. Harrison, and J. H. Kehrl. 2009. TLR4 signaling augments B lymphocyte migration and overcomes the restriction that limits access to germinal center dark zones. *J. Exp. Med.* 206: 2641–2657.
10. Kawai, T., and S. Akira. 2010. The role of pattern-recognition receptors in innate immunity: update on Toll-like receptors. *Nat. Immunol.* 11: 373–384.
11. West, M. A., R. P. Wallin, S. P. Matthews, H. G. Svensson, R. Zaru, H. G. Ljunggren, A. R. Prescott, and C. Watts. 2004. Enhanced dendritic cell antigen capture via toll-like receptor-induced actin remodeling. *Science* 305: 1153–1157.
12. Faure-André, G., P. Vargas, M. I. Yuseff, M. Heuzé, J. Diaz, D. Lankar, V. Steri, J. Manry, S. Hugues, F. Vascotto, et al. 2008. Regulation of dendritic cell migration by CD74, the MHC class II-associated invariant chain. *Science* 322: 1705–1710.
13. Lokuta, M. A., and A. Huttenlocher. 2005. TNF-alpha promotes a stop signal that inhibits neutrophil polarization and migration via a p38 MAPK pathway. *J. Leukoc. Biol.* 78: 210–219.
14. Yi, L., P. Chandrasekaran, and S. Venkatesan. 2012. TLR signaling paralyzes monocyte chemotaxis through synergized effects of p38 MAPK and global Rap-1 activation. *PLoS ONE* 7: e30404.
15. Bajénoff, M., J. G. Egen, L. Y. Koo, J. P. Laugier, F. Brau, N. Glaichenhaus, and R. N. Germain. 2006. Stromal cell networks regulate lymphocyte entry, migration, and territoriality in lymph nodes. *Immunity* 25: 989–1001.
16. Cyster, J. G. 2010. B cell follicles and antigen encounters of the third kind. *Nat. Immunol.* 11: 989–996.
17. Sáez de Guinoa, J., L. Barrio, M. Mellado, and Y. R. Carrasco. 2011. CXCL13/CXCR5 signaling enhances BCR-triggered B-cell activation by shaping cell dynamics. *Blood* 118: 1560–1569.
18. Nagai, Y., R. Shimazu, H. Ogata, S. Akashi, K. Sudo, H. Yamasaki, S. Hayashi, Y. Iwakura, M. Kimoto, and K. Miyake. 2002. Requirement for MD-1 in cell surface expression of RP105/CD180 and B-cell responsiveness to lipopolysaccharide. *Blood* 99: 1699–1705.
19. Divanovic, S., A. Trompette, L. K. Petiniot, J. L. Allen, L. M. Flick, Y. Belkaid, R. Madan, J. J. Haky, and C. L. Karp. 2007. Regulation of TLR4 signaling and the host interface with pathogens and danger: the role of RP105. *J. Leukoc. Biol.* 82: 265–271.
20. Adachi, O., T. Kawai, K. Takeda, M. Matsumoto, H. Tsutsui, M. Sakagami, K. Nakanishi, and S. Akira. 1998. Targeted disruption of the MyD88 gene results in loss of IL-1- and IL-18-mediated function. *Immunity* 9: 143–150.
21. Hoebe, K., X. Du, P. Georgel, E. Janssen, K. Tabeta, S. O. Kim, J. Goode, P. Lin, N. Mann, S. Mudd, et al. 2003. Identification of Lps2 as a key transducer of MyD88-independent TIR signalling. *Nature* 424: 743–748.
22. Kuma, Y., G. Sabio, J. Bain, N. Shpiro, R. Márquez, and A. Cuenda. 2005. BIRB796 inhibits all p38 MAPK isoforms in vitro and in vivo. *J. Biol. Chem.* 280: 19472–19479.
23. Carrasco, Y. R., S. J. Fleire, T. Cameron, M. L. Dustin, and F. D. Batista. 2004. LFA-1/ICAM-1 interaction lowers the threshold of B cell activation by facilitating B cell adhesion and synapse formation. *Immunity* 20: 589–599.
24. Huang, C., K. Jacobson, and M. D. Schaller. 2004. MAP kinases and cell migration. *J. Cell Sci.* 117: 4619–4628.
25. Jaffe, A. B., and A. Hall. 2005. Rho GTPases: biochemistry and biology. *Annu. Rev. Cell Dev. Biol.* 21: 247–269.
26. Heasman, S. J., and A. J. Ridley. 2008. Mammalian Rho GTPases: new insights into their functions from in vivo studies. *Nat. Rev. Mol. Cell Biol.* 9: 690–701.

27. Takenawa, T., and H. Miki. 2001. WASP and WAVE family proteins: key molecules for rapid rearrangement of cortical actin filaments and cell movement. *J. Cell Sci.* 114: 1801–1809.
28. Kong, L., and B. X. Ge. 2008. MyD88-independent activation of a novel actin-Cdc42/Rac pathway is required for Toll-like receptor-stimulated phagocytosis. *Cell Res.* 18: 745–755.
29. Troutman, T. D., W. Hu, S. Fulenchek, T. Yamazaki, T. Kurosaki, J. F. Bazan, and C. Pasare. 2012. Role for B-cell adapter for PI3K (BCAP) as a signaling adapter linking Toll-like receptors (TLRs) to serine/threonine kinases PI3K/Akt. *Proc. Natl. Acad. Sci. USA* 109: 273–278.
30. So, L., and D. A. Fruman. 2012. PI3K signalling in B- and T-lymphocytes: new developments and therapeutic advances. *Biochem. J.* 442: 465–481.
31. Jabara, H. H., D. R. McDonald, E. Janssen, M. J. Massaad, N. Ramesh, A. Borzutzky, I. Rauter, H. Benson, L. Schneider, S. Baxi, et al. 2012. DOCK8 functions as an adaptor that links TLR-MyD88 signaling to B cell activation. *Nat. Immunol.* 13: 612–620.
32. Pearce, G., T. Audzevich, and R. Jessberger. 2011. SYK regulates B-cell migration by phosphorylation of the F-actin interacting protein SWAP-70. *Blood* 117: 1574–1584.
33. Spaargaren, M., E. A. Beuling, M. L. Rurup, H. P. Meijer, M. D. Klok, S. Middendorp, R. W. Hendriks, and S. T. Pals. 2003. The B cell antigen receptor controls integrin activity through Btk and PLCgamma2. *J. Exp. Med.* 198: 1539–1550.
34. Gantner, B. N., R. M. Simmons, S. J. Canavera, S. Akira, and D. M. Underhill. 2003. Collaborative induction of inflammatory responses by dectin-1 and Toll-like receptor 2. *J. Exp. Med.* 197: 1107–1117.
35. Bone, H., and N. A. Williams. 2001. Antigen-receptor cross-linking and lipopolysaccharide trigger distinct phosphoinositide 3-kinase-dependent pathways to NF-kappa B activation in primary B cells. *Int. Immunol.* 13: 807–816.
36. Liu, X., B. Ma, A. B. Malik, H. Tang, T. Yang, B. Sun, G. Wang, R. D. Minshall, Y. Li, Y. Zhao, et al. 2012. Bidirectional regulation of neutrophil migration by mitogen-activated protein kinases. *Nat. Immunol.* 13: 457–464.
37. Benvenuti, F., S. Hugues, M. Walmsley, S. Ruf, L. Fetler, M. Popoff, V. L. Tybulewicz, and S. Amigorena. 2004. Requirement of Rac1 and Rac2 expression by mature dendritic cells for T cell priming. *Science* 305: 1150–1153.
38. Wu, Y. I., D. Frey, O. I. Lungu, A. Jaehrig, I. Schlichting, B. Kuhlman, and K. M. Hahn. 2009. A genetically encoded photoactivatable Rac controls the motility of living cells. *Nature* 461: 104–108.